Nanoarchitectures of semiconducting and piezoelectric zinc oxide

Pu Xian Gao and Zhong L. Wang[a)]
School of Materials Science and Engineering, Georgia Institute of Technology, Atlanta, Georgia 30332-0245

(Received 29 September 2004; accepted 16 November 2004; published online 21 January 2005)

Semiconducting and piezoelectric zinc oxide has two important structure characteristics: the multiple and switchable growth directions: $\langle 01\bar{1}0\rangle$, $\langle 2\bar{1}\bar{1}0\rangle$, and $\langle 0001\rangle$; and the $\{0001\}$ polar surfaces. The fast growth directions create nanobelts of different crystallographic facets, and the polar surfaces result in bending of the nanobelt for minimizing the spontaneous polarization energy. A combination of these distinct growth characteristics results in a group of unique nanostructures, including several types of nanorings, nanobows, platelet circular structures, Y-shape split ribbons, and crossed ribbons. We present here the as-grown nanoarchitectures naturally created by combining some of the fundamental structure configurations of ZnO, which could be unique for many applications in nanotechnology. © *2005 American Institute of Physics*. [DOI: 10.1063/1.1847701]

I. INTRODUCTION

ZnO is an important semiconducting and piezoelectric material that has versatile applications in the field of optoelectronics, piezoelectric sensors, transducers, and resonators. For the sake of lacking the central symmetry in wurtzite, combined with a large electromechanical coupling, ZnO exhibits strong piezoelectric and pyroelectric properties, and is ideally suitable for applications in sensors and actuators. Optically, ZnO is a wide-band-gap compound semiconductor that is suitable for short-wavelength optoelectronic applications. The high exciton binding energy (60 meV) in a ZnO crystal can ensure an efficient excitonic emission at room temperature, and room-temperature ultraviolet (UV) luminescence has been reported in disordered nanoparticles and thin films. ZnO is transparent to visible light and can be made highly conductive by doping.

As a wurtzite-structured oxide, zinc oxide is of three types and a total of 13 fastest growth directions: $\langle 0001\rangle$, $\langle 01\bar{1}0\rangle$, $\langle 2\bar{1}\bar{1}0\rangle$. Together with a pair of polar-surfaces $\{0001\}$, such a uniquely structured material has been demonstrated to form a diversity group of nanostructures, including nanobelts,[1] nanocombs,[2] nanosprings,[3] nanorings,[4] nanobows,[5] nanojunction arrays,[6,7] and nanopropeller arrays,[8] which are formed largely due to the high ionicity of the polar surfaces (for reviews, see Refs. 9 and 10). The branching growth phenomena, such as nanojunction arrays[6,7] and nanopropeller arrays,[8] have attracted great interest for achieving high degree of superior functionality via direct hierarchical self-assembly.[8,11]

In this paper, using a solid-vapor phase process, a group of unique nanoarchitectures of ZnO is synthesized, including several types of nanorings, platelet circular structures, Y-shape split ribbons, and crossed ribbons. The structures of these as-grown products have been analyzed and their formation processes are presented. These complex growth configurations are composed of some of the fundamental components, such as nanorod, nanobelt, and nanoring, and they could have unique applications in nanotechnology.

II. POLAR-SURFACES-INDUCED TYPICAL NANOSTRUCTURE CONFIGURATIONS

Wurtzite zinc oxide has a hexagonal structure (space-group *C6mc*) with lattice parameters $a=0.3296$ and $c=0.52065$ nm. The structure of ZnO can be simply described as a number of alternating planes composed of tetrahedrally coordinated O^{2-} and Zn^{2+} ions, stacked alternatively along the *c* axis [Fig. 1(a)]. The tetrahedral coordination in ZnO results in a noncentral symmetric structure, and consequently, the piezoelectricity and pyroelectricity. Another important characteristic of ZnO is the polar surfaces. The most common polar surface is the basal plane. The oppositely charged ions produce positively charged Zn-(0001) and negatively charged O-$(000\bar{1})$ surfaces, resulting in a normal dipole moment and spontaneous polarization along the *c* axis.

For the (0001) polar-surface-dominated nanobelt, its structure can be approximated to be a capacitor with two parallel charged plates [Fig. 1(b)]. The polar nanobelt tends to roll over into an enclosed ring to reduce the electrostatic energy.[3] A spiral shape is also possible for reducing the electrostatic energy. The formation of the nanorings and nanohelixes can be understood from the nature of the polar surfaces. If the surface charges are uncompensated during the growth, the spontaneous polarization induces electrostatic energy due to the dipole moment, but rolling up to form a circular ring would minimize or neutralize the overall dipole moment, reducing the electrostatic energy. On the other hand, bending of the nanobelt produces elastic energy. The stable shape of the nanobelt is determined by the minimization of the total energy contributed by spontaneous polarization and elasticity. If the nanobelt is rolled uniradically loop by loop, the repulsive force between the charged surfaces stretches the nanohelix, while the elastic deformation force pulls the loops

[a)]Author to whom correspondence should be addressed; electronic mail: zhong.wang@mse.gatech.edu

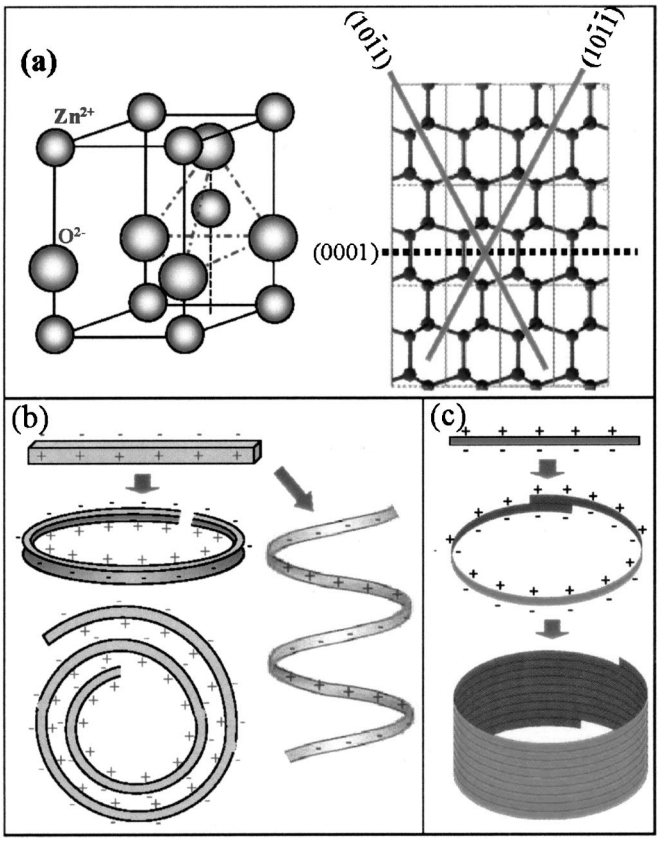

FIG. 1. (Color online) (a) Three-dimensional structure model of the unit cell of ZnO, and the corresponding projection along the *a* axis, showing the polar surfaces terminated with Zn and O, respectively. (b) Schematic model of a polar nanobelt, and the possible nanostructures created by folding the polar nanobelt with its polar direction pointing towards the center, forming nanoring, nanospiral, and nanohelixes. (c) Model of a polar nanobelt and its self-coiling process for forming a multilooped ring by folding the nanobelt with its polar direction pointing to the axial direction of the ring. The nanoring is initiated by folding a nanobelt into a loop with overlapped ends due to the long-range electrostatic interaction among the polar charges; the short-range chemical bonding stabilizes the coiled ring structure; and the spontaneous self-coiling of the nanobelt is driven by minimizing the energy contributed by polar charges, surface area, and elastic deformation.

together; the balance between the two forms the nanohelix/nanospring. In all of the cases illustrated here, the polar-axis *c* is pointing towards the center.

A different structure configuration is introduced, if the direction of the spontaneous polarization is rotated for 90°. The nanobelt has polar charges on its top and bottom surfaces [Fig. 1(c)]. If the surface charges are uncompensated during growth, the nanobelt may tend to fold itself as its length gets longer to minimize the area of the polar surface. One possible way is to interface the positively charged Zn-$(000\bar{1})$ plane (top surface) with the negatively charged O-$(000\bar{1})$ plane (bottom surface), resulting in neutralization of the local polar charges and the reduced surface area, thus forming a loop with an overlapped end. The long-range electrostatic interaction is likely to be the initial driving force for folding the nanobelt to form the first loop for the subsequent growth. As the growth continues, the nanobelt may be naturally attracted onto the rim of the nanoring due to electrostatic interaction and extends parallel to the rim of the nanoring to neutralize the local polar charge and reduce the surface area, resulting in the formation of a self-coiled, coaxial, uniradius, and multilooped nanoring structure.[4]

Structurally, ZnO has three types of fast growth directions: $\langle 2\bar{1}\bar{1}0\rangle$ $(\pm[2\bar{1}\bar{1}0], \pm[\bar{1}2\bar{1}0], \pm[\bar{1}\bar{1}20])$; $\langle 01\bar{1}0\rangle \times(\pm[01\bar{1}0], \pm[10\bar{1}0], \pm[1\bar{1}00])$; and $\pm[0001]$. Together with the polar surfaces due to atomic terminations, ZnO exhibits a wide range of unique structures that can be grown by tuning the growth rates along these directions. These are the fundamental principles understanding the formation of numerous ZnO nanostructures.

III. EXPERIMENT

A high-temperature solid-vapor deposition process was used to grow the unique piezoelectric nanostructures of ZnO reported here. The solid-vapor deposition involves using an experimental setup consisting of a horizontal high-temperature tube furnace with a length of ~50 cm, an alumina tube (~75 cm in length), a rotary pump system, and a gas controlling system. Commercial (Alfa Aesor) ZnO as the source materials was loaded on an alumina boat and positioned at the center of the alumina tube, the highest temperature zone. The process was conducted at 1370 °C for 120 min under a pressure of ~200 mbar. The Ar carrier gas flow rate is controlled at 50 sccm (standard cubic centimeters per minute). The as-grown nanostructures were collected on the polycrystalline Al_2O_3 substrate in the high-temperature region of ~900 °C.

Scanning electron microscopy (SEM) (field-emission LEO 1530 FEG at 5 and 10 kV), transmission electron microscopy (TEM) (field-emission TEM Hitachi HF-2000 at 200 kV), and energy-dispersive x-ray spectroscopy (EDS) attached to the SEM and TEM, respectively, were used to investigate the morphology, crystal structure, and composition of as-grown nanostructures.

IV. RESULTS AND DISCUSSION

The as-synthesized samples exhibit a wide range of nanostructures. After a systematic examination of the grown sample by SEM, we have classified the nanostructures into several groups, which will be described in detail in the following sections.

A. Circular architectures

The first group of rings is rooted from the alumina substrate. Figure 2(a) is a typical SEM image showing two thin and straight belts (ribbons), about 1–2 μm in width and ~10 μm in length, lying on an Al_2O_3 substrate. Both ends of the ribbons are of a symmetrical triangular shape. The TEM image and diffraction indicate that the ribbon is dominated by the flat $\{0001\}$ facets, with growth direction $[01\bar{1}0]$ and side surfaces $\pm(2\bar{1}\bar{1}0)$. The two side facets of the triangular tip are the $(10\bar{1}0)$ and $(\bar{1}100)$ facets. Figures 2(c)–2(f) are the four typical SEM images of the rings created by self-bending during growth to reduce the energy of spontaneous polarization. The rings were initiated from the alumina substrate and ended at the substrate as well. In Fig. 2(c), a top view indicates that the belt apparently started growth from a ZnO nanoisland (as indicated by an arrowhead). A uniform bend-

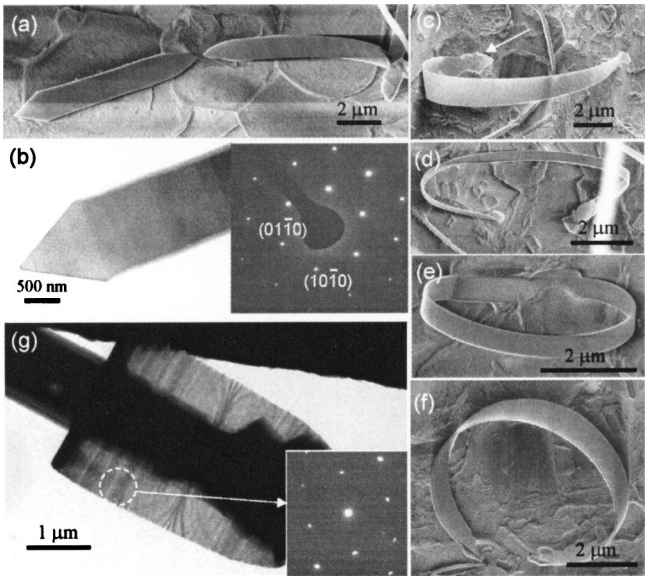

FIG. 2. (a) SEM image of two freestanding ZnO straight ribbons with triangular-shaped tips. (b) TEM image of a triangular tip terminated ribbon; the inset diffraction pattern shows that the ribbon is dominated by {0001} and the growth direction is [01$\bar{1}$0]. (c), (d), (e) and (f) are SEM images of a semiring, three-quarter ring, top view of a full ring, and side view of a nearly full ring rooted at Al_2O_3 substrate, respectively. (g) A typical TEM image of a micron-sized ring and the corresponding electron-diffraction pattern from the dotted circle area, indicating the tangential direction of the ring is [01$\bar{1}$0].

ing of the smooth belt forms a semiring, and the initial triangular growth tip finally ends the growth at another nanoisland on the substrate. The width of the ring is 1–3 μm. The coiling radius is 3–5 μm. Similarly, from the side view, a three-quarter nanoring is rooted at the substrate [Fig. 2(d)], which has a dimension of 300–400 nm in width and ~4 μm in radius. Figure 2(e) is a side view image of a nearly full-ring structure rooted at the substrate. Figure 2(f) shows another nearly full ring rooted at the alumina substrate. The circular shape is almost perfectly preserved. The triangular tip is clearly seen. To verify the crystal structure of the rings formed by straight triangular tipped ribbons, a TEM image of a ZnO ring is shown in Fig. 2(g). The contrast pattern shown on the ring surface is due to the strain contract introduced by bending. A selective area diffraction pattern recorded from the side of the nanoring indicates its single-crystal structure and the large surface is dominated by {0001}. The formation of the nanoring follows the model shown in Fig. 1(b).

The second group of rings is rooted at a ZnO crystal. Figure 3 presents a series of closed rings with different growth morphologies. Figure 3(a) is a nanoring coiled in a radius of ~4 μm and width of ~500 nm, and it is rooted at a side surface of a micro-ZnO rod. The morphology shown in Fig. 3(b) gives a good example of a nanobelt that switched its growth direction during the syntheses. The belt grew along a specific direction, then it switched at ~30° into another direction, and finally rotated 60° and then self-coiled into a full ring. The third morphology is shown in Fig. 3(c), where a nanoring is formed by at least two loops of a nanobelt closely stacking one onto the other due to the electrostatic forces induced by oppositely charged polar surfaces. Figure 3(d) is an example of self-coiled nanoring starting

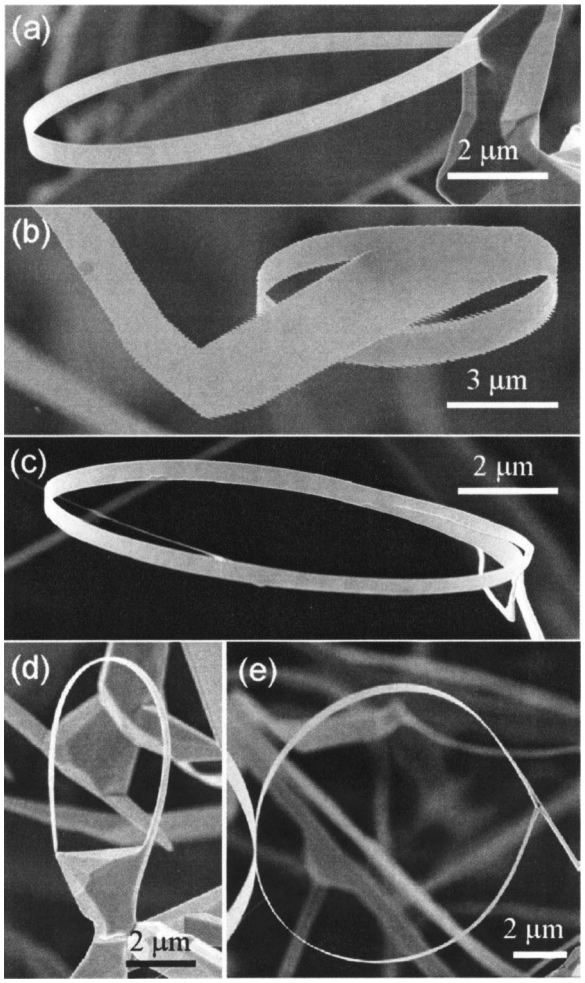

FIG. 3. A series of closed full rings with different growth configurations. (a) A nanoring started and ended at the same ZnO rod. (b) A nanoring formed after the nanobelt switching its growth direction. (c) A nanoring formed by a double-loop coiling of a nanobelt. (d) A nanobow started and ended at the two sides of a large crystal. (e) A nanobelt self-coiled into a nanoring with growth front rejoining the nanoribbon.

from a side surface of a ZnO rod, ending at a pyramid tip. Figure 3(e) describes a nanobelt with increasing thickness, thus, a ring is formed when the thickness is small, but it is too hard to bend when the thickness is larger. At the ending point, there is a ~60° joining angle between the belt-starting tip and stemmed ribbon to match the crystal symmetry.

An architecture can be made by combining the growth configurations presented in Figs. 1(b) and 1(c). Figure 4 is a combination of a nanorod, a semicircular bow, and a perfect ring. The nanorod grows along [0001] and is enclosed by six {01$\bar{1}$0} side facets. A nanobelt grows perpendicularly to the nanorod along [01$\bar{1}$0], bends uniformly, and finally ends at the nanorod, forming a nanobow.[5] This nanobelt is dominated by the {0001} polar surfaces and the polar charges enforce the bending of the nanobelt. The joint point between the nanobelt and the rod is a neck structure. A complete ring on the top of the nanorod has a solid conjunction with the rod, and its large surfaces are ±(01$\bar{1}$0), and its top and bottom rims are the {0001} polar surfaces. The growth direction of the self-coiled belt is [2$\bar{1}\bar{1}$0], similar to the seamless nanoring reported previously[4] [Fig. 1(c)].

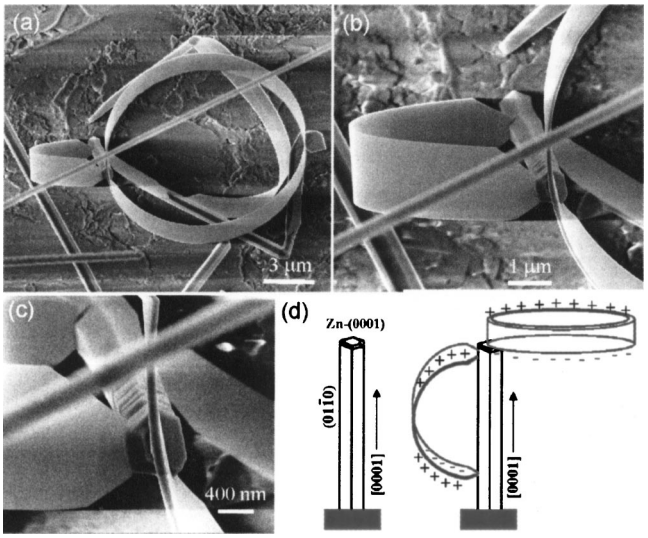

FIG. 4. (a) A nanoarchitecture composed of a rod, a bow, and a ring. (b,c) Magnified SEM images to capture the orientation relationships among the three components. (d) A structure model of the architecture.

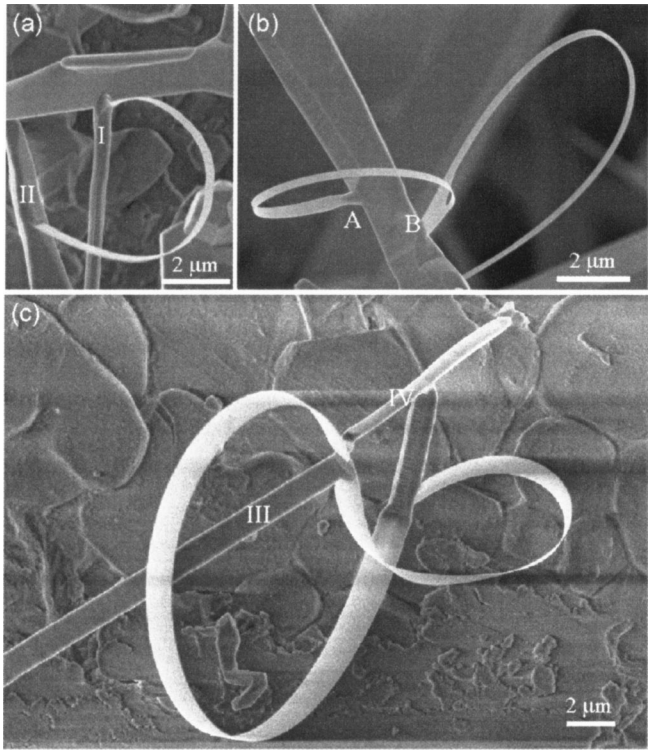

FIG. 5. (a) Polar nanobelt of uniform width that was initiated at one nanorod (I) and ended at another rod (II). (b) Conjunction of two nanorings. (c) A curved and twisted ZnO nanobelt that constructs architecture.

The combined growth structure presented in Fig. 4 is the first observation of its kind. This type of combination directly proves the coexistence of the polar belt rolled rings/bow and the polar belt self-coiled seamless nanoring. Figure 4(d) is a schematic model for this integrated growth phenomenon. The first step is a growth of a hexagonal rod along [0001]. The top facet is dominated by Zn-terminated (0001) plane, which is self-catalytically active,[2] and the side facets are likely to be the six crystallographically equivalent $\{01\bar{1}0\}$ surfaces. As growth continues, the stepped side facets, as shown in Fig. 4(c), would function as a good nucleation site for the secondary growth, leading to the formation of a belt along a normal direction of $[01\bar{1}0]$. Due to the spontaneous polarization of the ZnO nanobelt across its thickness, bending into a ring would reduce the electrostatic energy, provided the thickness-to-radius ratio is less than ~4%.[3,5] Bending is ended if the nanobelt reaches the rod and rejoins the single-crystal rod, forming a semicircular bow. On the other hand, with the growth of the rod, the growth front of Zn-(0001) plane could be the nucleation site for the other fast growth belts along $[2\bar{1}\bar{1}0]$ parallel to the side facet of the rod, and it tends to fold back to form a loop, such as the model shown in Fig. 1(c). A perfect ring is formed by epitaxial self-coiling of a polar belt.[4] The bottom surface of the ring tends to be O-$(000\bar{1})$ surface, while the top surface is Zn (0001).

The ending of a circularly bending nanobelt could be fairly complex and interesting. Figure 5 shows several cases that the rejoining position of a nanobelt could be its own crystal or another piece of crystal. For example, in Fig. 5(a), the polar nanobelt initiates its growth from one nanorod (I) and ends its growth at another rod (II), and the belt width keeps uniform around 500 nm. In Fig. 5(b), assuming the growth of the nanobelt starts from position A, which is along a direction parallel to the larger flat surface, the belt tends to reduce its electrostatic energy by self-bending and coiling into a spiral to touch the crystal at position B. As seen in Fig. 5(c), the nanobelt could twist itself into a configuration that matches the local crystallography and surface charge. Secondary growth is responsible for the unusual twisting configuration of the nanobelt.

B. Platelet nanoarchitectures

For the polar-surface-dominated platelet structure, a change in growth direction among the six crystallographic equivalent directions of $\langle 01\bar{1}0\rangle$ or $\langle 2\bar{1}\bar{1}0\rangle$ could give a diver group of nanostructures. Figures 6(a) and 6(b) show circular and planar rings, which are formed by switching the growth directions among $\langle 01\bar{1}0\rangle$, while keeping the large (0001) surface flat. Figure 6(c) is a case in which three branches grew first along three $\langle 01\bar{1}0\rangle$ directions, and then one of the two side branches crossed the middle branch underneath its surface, and then rejoin the other branch. The joining point is not flat due to the mismatch (as indicated by a dotted ellipse) caused by passing the middle branch. The structure of this kind is a pair of "bow and arrow." It is worth mentioning that such a combined structure is still a single crystal, although at the interface there is apparently a mismatch. Under TEM, it is found that the two side ribbons could miss each other at the joining point [Fig. 6(d)]. The inset diffraction pattern from the dotted circle area shows a single-crystal [0001] pattern, which reveals that the top and bottom surfaces are the {0001} polar surfaces. It must be pointed out that the planar circularlike structure presented here is formed by changing the growth direction among the six crystallographic equivalent directions, rather than the minimization of electrostatic energy.

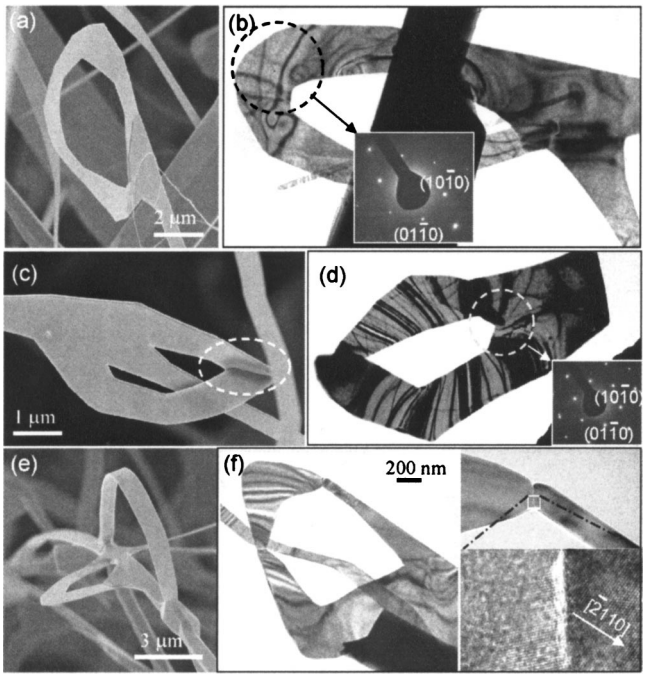

FIG. 6. Complex platelet circularly closed structures formed by changing the growth direction of the ribbon. (a,b) SEM image and TEM image of a planar polar-surface-dominated full-ring structure, respectively; the inset [0001] diffraction pattern is from the dotted circle area; (c) SEM image of a planar bow-arrow structure. The structure creates a displacement at the joining plane of the two side branches. (d) TEM image for a platelet structure and an electron-diffraction pattern recorded from the dotted circle area. (e) A combined structure of a polar ribbon, a platelet semicircle structure, and a uniform bow. (f) TEM image of a closed loop composed of three pieces of polar ribbon of different shapes. A high magnification TEM image and a high-resolution TEM image from the interface between the adjacent nanoribbons are given.

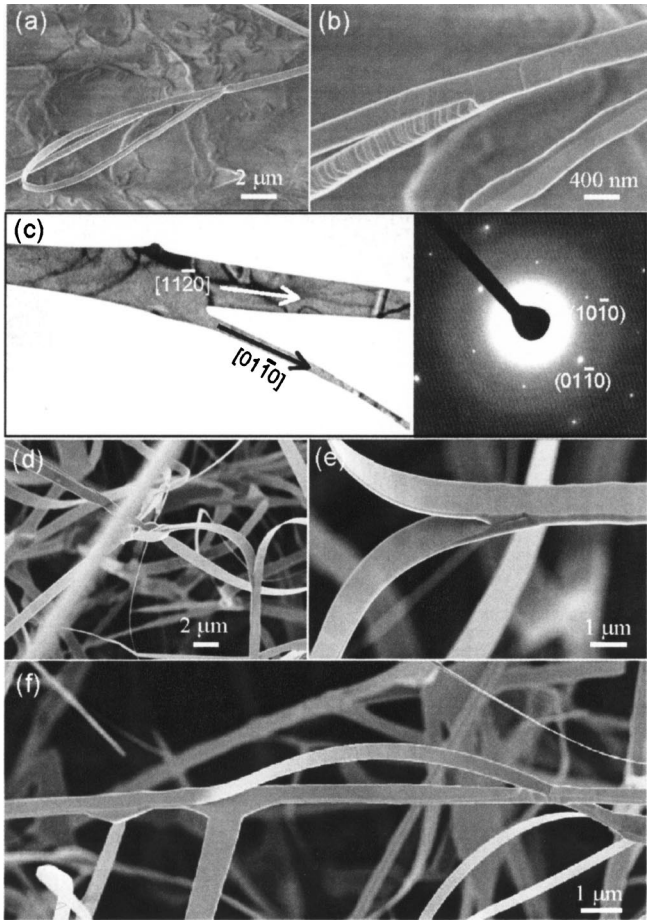

FIG. 7. (a,b) SEM images of a nanoring with one side having a split branch. (c) TEM image and corresponding [0001] diffraction pattern of a *Y* structure, which is produced by separating the growth along [01$\bar{1}$0] from the original [$\bar{2}$110] direction. (d,e) SEM images of two tangential split ribbons. (f) A bow structure formed by the split growth of a belt and its later rejoining to the straight ribbon.

A combination of the planar circular structure with the rings could form a complex nanoarchitecture. Figure 6(e) is a structure composed of a planar semicircle with a nanobow. The former is the result of unique crystallography with the polar axis pointing upwards, and the latter is due to spontaneous polarization with the polar axis pointing towards the center. The two semirings have complementary and coincident growth orientations with the connecting ribbon, forming a single-crystal piezoelectric ring structures.

In addition to the single-crystal circular structures, closed rings formed by connecting multiple crystals are also possible. Figure 6(f) is a TEM image of a closed loop by combination of three pieces of different shaped polar-surface-dominated nanoribbons. Although three of them have almost identical orientation, small angle interfaces are present among them. The inset high-resolution TEM image recorded from an interface reveals that the interface has a finite width. A coherent lattice match at the interface may be responsible for forming the tricrystal full circular structure.

C. Y-shape single-crystal nanoribbons

Splitting of a single crystal could occur and the side branch growth leads to the formation of Y-shape nanoarchitecture of ZnO. Figure 7 gives a typical example for the split growth phenomena. As shown in Fig. 7(a), a nanoring similar to the one described in Fig. 3(e) is formed. However, this nanoring is formed by a bigger and rougher nanoribbon. From the magnified picture presented in Fig. 7(b), it is seen that the exterior surface of the ring is smooth but the inner surface has steps, which indicates that the inner surface is Zn-(0001) surface and the exterior surface is O (000$\bar{1}$).[2] An important feature is that one side of the ring splits into two branches [Fig. 7(a)]. The TEM imaging and diffraction show that the splitting is due to an initiation of a side branch along [01$\bar{1}$0] away from the original branching direction of [11$\bar{2}$0], but both branches are still dominated by {0001} polar surfaces.

Figure 7(d) shows that a ribbon of large aspect ratio (around 5–10) and smooth polar surfaces splits into two high aspect ratio ribbons of equal width but half in thickness. The ribbon was too thick to be bent by polar charge prior splitting, but bending is possible after splitting [Fig. 7(e)]. Figure 7(f) shows that a curly ribbon splits out of a straight ribbon, later it rejoins the straight ribbon. The curly ribbon is due to its small thickness and is due to the surface polar charge. These growth features are rather unique.

Joining two nanostructures together could occur in two ways. One is a natural crystallographic matching so that two of them are integrated as a single crystal. The other is a

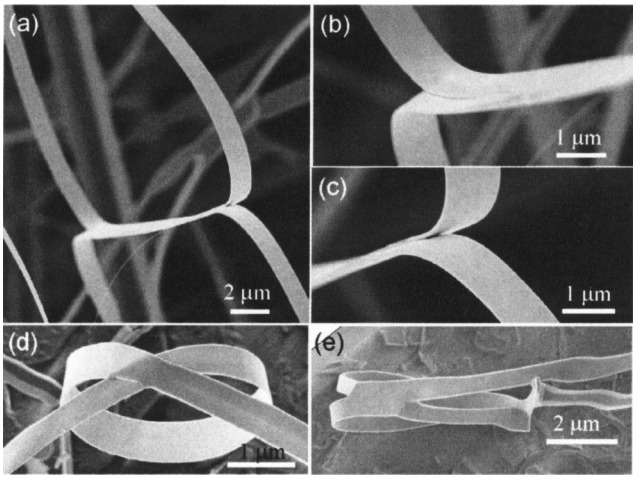

FIG. 8. Joining of nanostructures via high-temperature sintering. (a) Two micron-sized ribbons merged in parallel in the contact region, and (b,c) are the enlarged views of the left-hand and right-hand sides of the joining points, respectively. (d) A self-bent and twisted ribbon into a closed loop. (e) A polar-surface-dominated full-ring split out another nanoribbon, which overlapped and merged with the original loop.

sintering during growth. Figures 8(a)–8(c) show two nanobelts that are joined together. It is possible that both crystallographic bonding and sintering play a role in holding them together. But a case shown in Fig. 8(d) is likely due to sintering. The nanostructure shown in Fig. 8(e) is a result of self-splitting.

D. Crossed nanoribbon architectures

Crossed ribbon structures have been observed with some unusual configurations. One way of creating crossed structures is the switching/splitting in the growth directions among $\langle 01\bar{1}0\rangle$ and $\langle 2\bar{1}\bar{1}0\rangle$. These types of structures usually have a smooth surface and all of the branches share the same flat {0001} surface [Figs. 9(a) and 9(b). The two-branched nanoribbon in Fig. 9(c) grow along $[1\bar{2}10]$ and $[2\bar{1}\bar{1}0]$. For the three-branched nanoribbons in Fig. 9(d), electron-diffraction pattern shows that the three nanoribbons are a single crystal and are along $[\bar{1}100]$, $[01\bar{1}0]$, and $[\bar{1}010]$.

The other group of crossed structure is complex because there is a crystal at the joint point of the nanobelts, and sometimes the two nanobelts do not share a common flat surface [Figs. 9(e)–9(g). This type of structure could involve the formation of twins at the central crystal and/or sintering.[12] The two ribbons could grow perpendicularly from a cross-junction area, and they do not share a common flat surface. Figure 9(h) is a more complicated case, where multiple ribbons grew from one junction, forming a three-dimensional (3D) complex structure. These nanostructures demonstrate the diversity of ZnO growth.

E. Zig-zag chain architectures

Zig-zag chain type of nanostructures have also been found for ZnO. Figure 10 shows two typical configurations of the zig-zag structures. The chain structures are dominated by the large {0001} polar surfaces, but its growth direction changes periodically, as shown in Fig. 10(c), leading to the

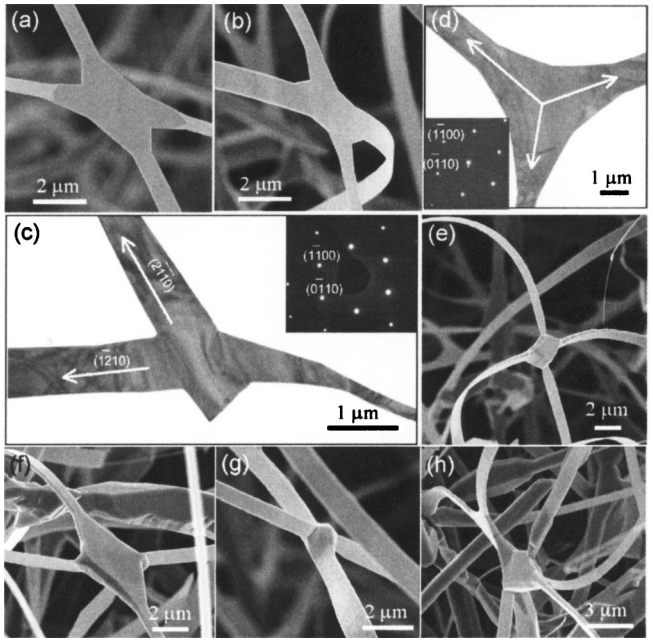

FIG. 9. Crossed junctions of ZnO. (a–d) SEM and TEM images of the crossed nanobelts that share the same polar surface of (0001). The junction branches could be along $[01\bar{1}0]$ or $[2\bar{1}\bar{1}0]$. (e–g) Cross junctions of nanobelts with twisted ribbons, so that they do not share a common polar surface. (h) A multijunction structure of over four ribbons.

formation of chain structures. For the same family of growth directions of $\langle 01\bar{1}0\rangle$, for example, there are six equivalent directions and there is a 60° rotation between the two adjacent directions. Therefore, a periodic change in growth direction following a periodicity of $[\bar{1}100]\rightarrow[10\bar{1}0]\rightarrow[01\bar{1}0]$

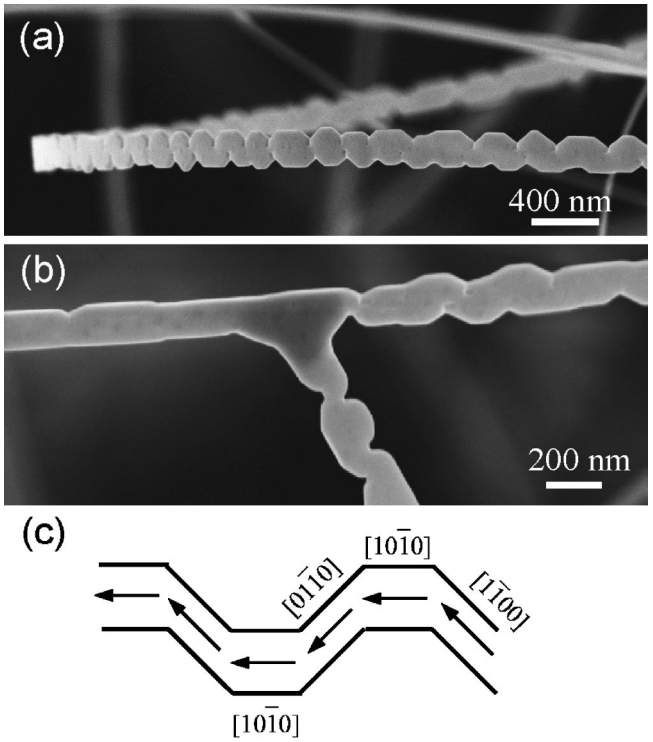

FIG. 10. (a,b) Polar-surface-dominated ZnO ribbons with zig-zag chain structure, which are formed by a periodic change in growth direction. (c) A model of the chain structure.

$\rightarrow[10\bar{1}0]$, and a fixed length growth results in the formation of zig-zag chain structure, similar to the one reported previously.[5] The junction shown in Fig. 10(b) is due to a split growth of the nanoribbon along one of the directions.

V. CONCLUSION

ZnO is a semiconducting and piezoelectric material that has important applications in optoelectronics, sensors and actuators. ZnO has two important structure characteristics: the multiple and switchable growth directions: $\langle 01\bar{1}0\rangle$, $\langle \bar{2}110\rangle$, and $\langle 0001\rangle$; and the $\{000\bar{1}\}$ polar surfaces. With the three types of stable facets of $\{01\bar{1}0\}$, $\{\bar{2}110\}$, and $\{0001\}$, the three types and 13 fastest growth directions create a lot of freedom for the growth morphology. Nanobelts of different crystal facets have been synthesized. Another key factor is the polar surfaces. The Zn-terminated $(000\bar{1})$ surface is positively charged, and the O-terminated (0001) surface is negatively charged, thus, there is a spontaneous dipole moment along the *c* axis. If the crystal thickness is large, the effect of the dipole is small, but once the nanobelt is as thin as ~10 nm, the spontaneous polarization can produce a few unusual growth features, such as nanorings, nanobows, nanohelixes, and nanospirals, which are the results of minimizing the electrostatic energy due to the polarization. In this paper, we have shown that these fundamental growth features coexist during the growth, and their recombination produces a diverse group of nanoarchitectures: including several types of nanorings, nanobows, platelet circular structures, Y-shape split ribbons, and crossed ribbons. We have described the structures of these architectures in detail and explained their possible growth processes. Our results clearly demonstrate that ZnO is probably the most configurationally rich family for nanostructures among all of the known materials. We believe that these nanostructures will be the fundamental components for fabricating semiconducting and piezoelectric nanodevices for applications in nanoeletronics, nanooptoelectronics, biomedical science, and environmental sciences.

ACKNOWLEDGMENTS

The authors thank the financial support of the NASA Vehicle Systems Program and Department of Defense Research and Engineering (DDR&E) and the Defense Advanced Research Projects Agency for support of this research. This material is based upon work supported by the Space and Naval Warfare Systems Center San Diego under Award No. N66001-04-1-8903. Any opinions, findings, conclusions, or recommendations expressed in this publication are those of the author(s) and do not necessarily reflect the views of the Space and Naval Warfare Systems Center San Diego.

[1] Z. W. Pan, Z. R. Dai, and Z. L. Wang, Science **291**, 1947 (2001).
[2] Z. L. Wang, X. Y. Kong, and J. M. Zuo, Phys. Rev. Lett. **91**, 185502 (2003).
[3] X. Y. Kong and Z. L. Wang, Nano Lett. **3**, 1625 (2003).
[4] X. Y. Kong, Y. Ding, R. S. Yang, and Z. L. Wang, Science **303**, 1348 (2004).
[5] W. Hughes and Z. L. Wang, J. Am. Chem. Soc. **126**, 2709 (2004).
[6] P. X. Gao and Z. L. Wang, J. Phys. Chem. B **106**, 12653 (2002).
[7] J. Y. Lao, J. G. Wen, and Z. F. Ren, Nano Lett. **2**, 1287 (2002).
[8] P. X. Gao and Z. L. Wang, Appl. Phys. Lett. **84**, 2883 (2004).
[9] Z. L. Wang, J. Phys.: Condens. Matter **16**, R829 (2004).
[10] Z. L. Wang, X. Y. Kong, Y. Ding, P. X. Gao, W. L. Hughes, R. S. Yang, and Y. Zhang, Adv. Funct. Mater. **14**, 943 (2004).
[11] Z. L. Wang and Z. C. Kang, *Functional and Smart Materials—Structure Evolution and Structure Analysis* (Plenum, New York, 1998).
[12] Y. Dai, Y. Zhang, and Z. L. Wang, Solid State Commun. **126**, 629 (2003).